Sanchez-Sobrado *et al.*
Functional Composite Materials (2023) 4:2
https://doi.org/10.1186/s42252-023-00039-x

Functional Composite Materials

RESEARCH

Open Access

Evaluation of conductive smart composite polymeric materials for potential applicationsin structural health monitoring and strain detection

Olalla Sanchez-Sobrado*, Daniel Rodriguez, Ricardo Losada and Elena Rodriguez

Abstract

The presented work collects results from the evaluation of electrical response to mechanical deformation and formation of defects presented by different polymeric based composite materials with potential for applications in Structural Health Monitoring and Strain Detection. With the aim of showing the variety of key materials in sectors like civil aviation, wind energy, automotive or railway that present this ability, specimens of very different nature have been analyzed: a) thermoplastic commercial 3D printing filaments loaded with carbonic fillers; b) epoxy resin loaded with Carbon Nanotubes and c) long carbon fiber reinforced resin composite. Measurements of electrical properties of these materials were taken to evaluate their capability to detect the presence of structural defects of different sizes as well as its spatial location. On the other hand, simultaneous measurements of electrical resistivity and mechanical strain during tensile tests were performed to analyze the potential of materials as strain detectors. All composites studied have shown a positive response (modification of electrical performance) to external mechanical stimulus: induced damage and deformations.

Keywords Conductive composites, Structural health monitoring, Strain detection, Carbonic materials, Carbon nanotubes

*Correspondence:
Olalla Sanchez-Sobrado
olalla.sanchez@aimen.es
Full list of author information is available at the end of the article

Graphical Abstract

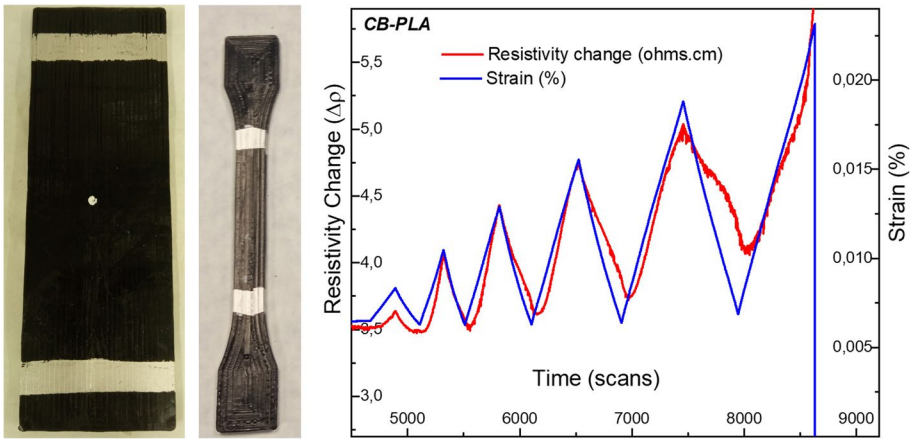

Introduction

Structural maintenance in several industrial sectors like civil aviation, wind energy, automotive or railway is being currently based on scheduled maintenance on-ground inspections, in which Non-Destructive Inspections (NDI) are used to detect damage within the structural materials. In this scenario, in-service Structural Health Monitoring (SHM) of composite material parts plays a key role in the assessment of their performance and structural health [1]. Conductive carbon-based materials networks like those based in carbon nanotubes (CNTs) and others have been recently utilized as in situ sensors to detect microcracking and deformations in polymer and fiber reinforced polymer composite materials by using resistivity change method [2, 3]. The low electrical percolation threshold of these conductive materials allows forming an electrically conductive network within the composite structure. This network allows the identification of the formation of microcracks due to the changes in the electrical resistance as well as the detection of mechanical deformations of the structure [4].

The resistivity change method to perform SHM is based in the fact that the generation of a microcrack in the polymer matrix of a composite material breaks conducting chains in the percolating conductive material or nanofiller network producing a modification on the electrical resistivity that can be related with the formation and size of the produced crack [5]. However, the spatial localization remains difficult. To overcome this drawback, resistance maps have been proposed to locate damage position [6] together with multi-scale modelling approach for simulating crack sensing [7]. On the other hand, the use of the coupled electro-mechanical response of these materials to self-sense their strain and damage during mechanical loading has been also widely studied [8]. Carbonic materials like CNTs (but not only) have been deeply analyzed as candidate for strain and motion sensors at the macroscale, due to the dependence of the electrical properties on mechanical deformation at the nanoscale due to piezoresistive behavior. Many publications report the use of this carbonic based polymer nanocomposite for in textile-based, wearable sensing system for real-time motion detection [9], muscle, breathing and pulse motion [10] or electronic skins [11]. Other different polymer/nano reinforcement combinations can inspire these applications. In this context, some important works reports remarkable advancements specially concerning the use of elastomeric materials as matrix due to their high response to external mechanical stimuli. D.Xiang et al. [12] produced highly flexible strain sensors of CNT/TPU nanocomposites by 3D printing sensors with significantly improved tensile and electrical properties (GF = 117,213 at a strain of 250%) by modifying the CNTs with 1-pyrenecarboxylic acid (PCA) which improves the polymer-nanofiller interactions. In other work, B. Podsiadły et al. [13] developed composite conductive fibers to be used in textronic systems based in flexible SBS polymer and different types of functional phases (CNTs, graphite, and a mixture of these carbon structures). 3D printing technologies were also selected by J.F.Christ et al. [14] to validate multiwalled carbon nanotube/thermoplastic polyurethane nanocomposites as strain sensors. Despite that elastomeric based conductive composite materials are the type with better prospective considering applications in strain sensing due to their huge stretchability, the inclusion of this kind of

smart materials with capacity to self-sense the structural health are acquiring more and more importance due to their potentiality to substitute sensing devices which often bring serious structural defects when integrating in the structures to be sensed during fabrication processes or are not able to access the interior of materials. Many important industrial sectors like aeronautics, civil construction or wind, which involve polymeric materials and composites with high mechanical performance, are currently seeking for these new intelligent materials that allows, not only to sense the formation of microcracks but also to obtain information of deformation that allow to feed digital twins to develop predictive model that led to maintenance costs reduction, which is a common critical point in this area [15, 16]. That is why we consider the material evaluation presented in this work very relevant.

In the presented work, electrical properties, and both damage and strain dependent electrical resistance characteristics of several different carbon-based/polymer composite and nanocomposite materials were investigated: (a) different carbon-based nano additives thermoplastic composite for 3D printing technologies: PLA/CB; ABS/CNTs; PETG/CNTs and PEKK/CNTs, which are nowadays highly considered for applications in numerous industrial sectors like aeronautics, wind energy, automotive, health, construction, or railway (b) CNTs reinforced RTM6 Epoxy resin and (c) long carbon fiber composite laminates. To analyze the ability of the different developed materials to detect different structural defects, the evolution of the electrical resistance when the size of the produced defect is increased has been analyzed for each composite. Systematically, large, and linear enhancement is obtained, even for the smallest defects. This behavior places polymeric composites integrating carbonic materials and nanomaterials as one of the most promising solutions for SHM applications. Some preliminary tests to evaluate capacities for failure detection have been as well performed. On the other hand, in this work we show a study of the capabilities presented by reinforced polymeric composites for strain detection. Simultaneous measurements of strain and electrical resistance were taken for representative composite coupons during tensile tests. The signal-matching presented by the different materials has been discussed as a direct estimation of the capability for strain sensing and potential use for strain and motion detection applications.

Experimental

Fused Filament Fabrication three-dimensional (FFF 3D) printing manufacturing process.

Four dog-bone-type specimens and four rectangular specimens were printed for each of the four purchased commercial filaments described below. The printing machine used was a 3D printing: A2V4 printing machine (3nt r). We have selected this industrial equipment due to high performance and printing temperature required to print the polymers of our study. For these applications, temperature requirements above 380 degrees, must be reached, which desktop printers cannot achieve. Photographs of the two different types of samples made of thermoplastic polymer (PLA) used in this report are shown in Fig. 1: tensile coupons for strain detection experiments (a) and coupons to evaluate the evolution of electrical properties with the defect size increment (b). Table 1 collects some of most important parameters involved in printing process.

Epoxy resin with CNTs

Epocyl is the trade name of an epoxy resin with an indetermined load of CNTs that was purchased from Nanocyl. To prepare coupons, 95,25 g of Epocyl was stirred at 60 rpm in a mechanical blender at 85ºC machine for 15 min. Afterwards, a mixture of accelerator and hardener was used: 15 g of Aradur 1571 (50%)/ 15 g of Accelerator 1573 (50%). A catalyst mixture consisting in 24 parts of the mixture and 76 of resin were prepared. The catalyst mixture is heated slightly before hand-mix it

Fig. 1 Images of the two different type of coupons made of thermoplastic polymer (PLA): tensile coupons for strain detection experiments (**a**) and coupons to evaluate the evolution of electrical properties with the defect size increment (**b**)

Table 1 Parameters of printing process

Printed Material	Temperature	Printing Speed	Number of layers	Diameter of filaments
PLA	220	30 mm/s	2	2.85 mm
ESD safe ABS	245	30 mm/s	2	2.85 mm
CNT PETG	245	30 mm/s	2	2.85 mm
PEKK-ESD	380	30 mm/s	3	1.75 mm

well and is mixed with the resins. A batch of dog-bone test tubes for mechanical tests and a batch of rectangular (4×10 cm) tests to measure evolution of resistivity when the hole size increases gradually were prepared. This procedure was also used to fabricated samples with increase load of CNTs, in this case the original Epocyl resin (containing the load of CNTs) was diluted in different amounts of RTM6 epoxy resin (which does not contain CNTs) at 60 rpm in a mechanical blender at 85ºC machine for 15 min. Once all different preparations are complete, the coupons were fabricated by pouring the blends in silicon moulds and cured in an oven at 120ºC during 4h30 min.

Prepreg layup manufacturing process

The layers of Carbon Fiber prepreg, purchased from Toray, were cut manually (0º,90º, + 45º,-45º). To fabricate the laminate several steps were followed. First, a release agent was applied on the tool surface. The stack of plies was piled up manually. After the first ply was laid, debulking was made to ensure a good adhesion of the prepreg to the tool surface. The rest of the plies were positioned following the stacking sequence. Debulking was performed for each four plies or when wrinkles appeared during stacking. This step was accomplished by placing a non-perforated bleeder film and breather layer under a flexible vacuum bag, and by applying 0,9 bar of vacuum. After placing all the prepreg layers, the coupon was covered by a peel ply, a layer of perforated bleeder film and a non-woven breather cloth. Before introducing the coupon on the oven, a vacuum test was performed to check the bag's integrity. Afterwards, the coupon was left under vacuum following the programmed curing cycle (Table 1). After curing a demoulding phase was carried out. The surface of the laminate in contact with the glass part of the mould had a smoother surface after manufacturing while the other side, presents a rougher texture since this surface was in contact with the vacuum bag consumables (the peel ply left a rough surface after manufacturing).

Process temperature and process time are the two more relevant parameters in the three processes described in this work since they determine the consolidation and final mechanical properties of the manufactured coupons. Table 2 collects this information. In the case of Carbon fiber reinforced polymer composite, the fabrication is carried out by following a curing process consisting in a sequence of temperatures and times. All values of temperature and time were selected following the manufacturers of the commercial products indications.

Measurements of electrical properties

Once manufactured, two silver contacts of 1 cm thick and separated by 5 cm were painted directly on the polymeric surface of coupons and the ohmic resistance was measured using crocodiles with the acquirer system: Data acquisitor system Keysight DAQ970A with an integrated DAQ901A-20 channels armature multiplexer module. This system acquires simultaneously measurements of electrical resistance (applies a current of 1 mA and measures the voltage (V) obtaining ohmic resistance presented by the material (Ohm's law $V = IR$)) and mechanical strain produced during a tensile test to analyze the SHM behavior.

Production of defects

With the aim of analyze the potential of polymeric conductive materials for self-monitoring the produced damage, holes of gradually increased size were

Table 2 Process temperatures and times corresponding to the three different processes

Manufactured specimens	Process Temperatures	Process Time
3D printing commercial thermoplastic filaments with nano-carbonic additives	220ºC	30 min
Epoxy resin with CNTs	120ºC	4h30min
Carbon fiber reinforced polymer composite	Curing process: **1)** 6 h at 40ºC, **2)** ramp up to 1ºC/min up to 80ºC, **3)** 5 h at 80ºC, **4)** ramp up to 132ºC, **5)** 2 h at 132ºC and **6)** cool down to room temperature	

performed in the center of each sample (hole enlarged using different drill bits).

Estimation of Conductivity and resistivity

$$\text{Shape Factor (F)} = \text{S/L} = 2 \times 0,5/5\ (\text{mm})\ \text{F} = 0,002\ \text{m}$$
$$\text{Conductivity } \sigma = 1/\rho = 1/\text{R} * 0,02\ (\text{S/m}).$$

Tensile tests

They were carried out following the ASTM D3039/D3039M standard, the speed was 1 mm/min, 10 cycles of ascent and descent were carried out in displacement control until reach the target tensions of 50, 100, 150, 200, 250, 300, 350, 400, 450 and 500 MPa. The speed of the section from 0 to 50 MPa is carried out at 0.5 mm/min. The speed of the rest of the sections is 1 mm/min. Due to the placement of the sensors on the specimen, the transverse extensometer cannot be installed. The conductivity and tensile tests were performed in the laboratory at temperature and humidity conditions of 25ºC and 40% respectively.

Results and discussion

3D printing commercial thermoplastic filaments with nano-carbonic additives

Dumbbell-type specimens were printed for each of the four purchased filaments, commercial filaments are described in Table 3. These consist basically in thermoplastic-based polymers of different type and characteristics: PLA, ABS, PETG and PEKK. All studied materials presented electrical conductivity due to small loads of different carbonic-based fillers: carbon nanotubes (CNTs) and Carbon Black (CB). To evaluate their conductivity, measurements of electrical resistance were taken. The estimated values for conductivity calculated using procedure explained in experimental section, are presented in column 4 of Table 3.

Table 3 Thermoplastic based conductive polymeric filaments used to evaluate conductive, SHM and strain detection capacities

Coupon	Description	Supplier	Resistance (ohm)
PLA	Carbon Black (load 20%)	Protopasta	0,588E3
ESD safe ABS	Unknown load of MWCNTs	3DXSTAT	0,464E6
CNT PETG	Unknown load of CNTs	3DXSTAT	0,346E9
PEKK-ESD	Unknown load of CNTs	3DXSTAT ESD	48.5E6

All materials show gradual change (resistivity increase, conductivity decrease) with increasing defect size. Results corresponding to PLA, PTGE and ABS are shown in graphs displayed in Fig. 2. All materials respond positively to the formation of a defect so they could be proposed for SHM purposes, nevertheless and despite being the least conductive, CNT-PTGE is considered the best candidate since it presents the greatest change in conductivity. The reason to observe the results plotted in the graphs is the different nature of the carbonic based filler which give conductivity to the materials. The differences of size and, most important, geometry of CB and CNT determine the type of dispersion nets that these acquire in the polymeric matrix leading to two different types of conductivity nets, which explain the differences observed between the different materials analyzed. With this, the type of filler integrating the nanocomposite plays a key role in this performance. Depending on the type of filler, two behaviors are observed. A) *Linear behavior* like when carbon black is the conductive filler. In this case, the change in conductivity with the size of the defect remains linear for the whole range of defect-sizes evaluated. B) *Percolation behavior* like in the case of the CNTs used as fillers. In the second case, two regions can be set. Up to 5 mm slow fall. From 5 mm abrupt drop (optimum zone). In this region a small variation in the size of a produced defect leads to high conductivity change, the higher the change the easiest to detect so these types of materials (filled with CNTs) are optimum for SHM purpose for a large range of defect sizes but especially above 5 mm.

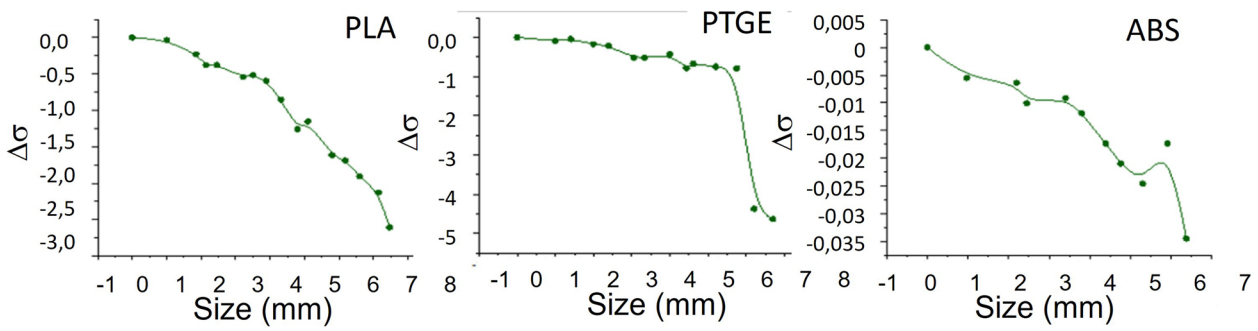

Fig. 2 Evolution of conductivity change with defect size for PLA, PTEG and ABS

For the four polymeric materials analysed, simultaneous measures were taken for the variation of the strain and the variation of electrical resistivity during a tensile test to evaluate the ability of these materials to detect mechanical deformation and evaluate their capacity for applications in strain detection. The results, shown in graphs of Fig. 3 are very satisfactory: for all materials, resistivity increases during deformation, and as soon as deformation ceases and the material returns to its original state, resistivity also decreases. As expected, when polymers reach their respective break point, bot curves resistivity change and strain collapses. All polymers analysed present have a similar value of elongation being PETG is the most "elastic", ABS is half elastic than PETG while PEKK is the one that endures more cycles as expected since it belongs to the polymer family known as “high performance polymers” characterized by their extraordinary mechanical properties. Beyond this, the different results obtained for the different materials analysed can be explaining considering their different mechanical properties: Polymer with better structural performances will reach higher number of load up and load down before break. As is widely known, PEKK is one of the highest mechanical properties thermoplastic polymers due to its extraordinary chemical stability, such properties are being already investigated for structural applications is sectors like aeronautics. This is clearly seen in the corresponding plot of Fig. 3. While PLA, ABS or PETG breaks after 6 cycles, PEEK resists up to 13 cycles of increasing load.

Epoxy resin with CNTs

With the aim of study, the percolation curve of epoxy resin loaded with an undetermined amount of CNTs, we prepared different blends of epoxy resin RTM6 and Epocyl resin containing the CNTs load. Results corresponding to the electrical conductivity of each are represented in Fig. 4a. The expected plateau after reaching maximum of percolation curve is not achieved even for the specimens containing a 100% of Epocyl resin which contains the load of CNTs. For the following experiments this was the blend selected. As shown in Fig. 4b,

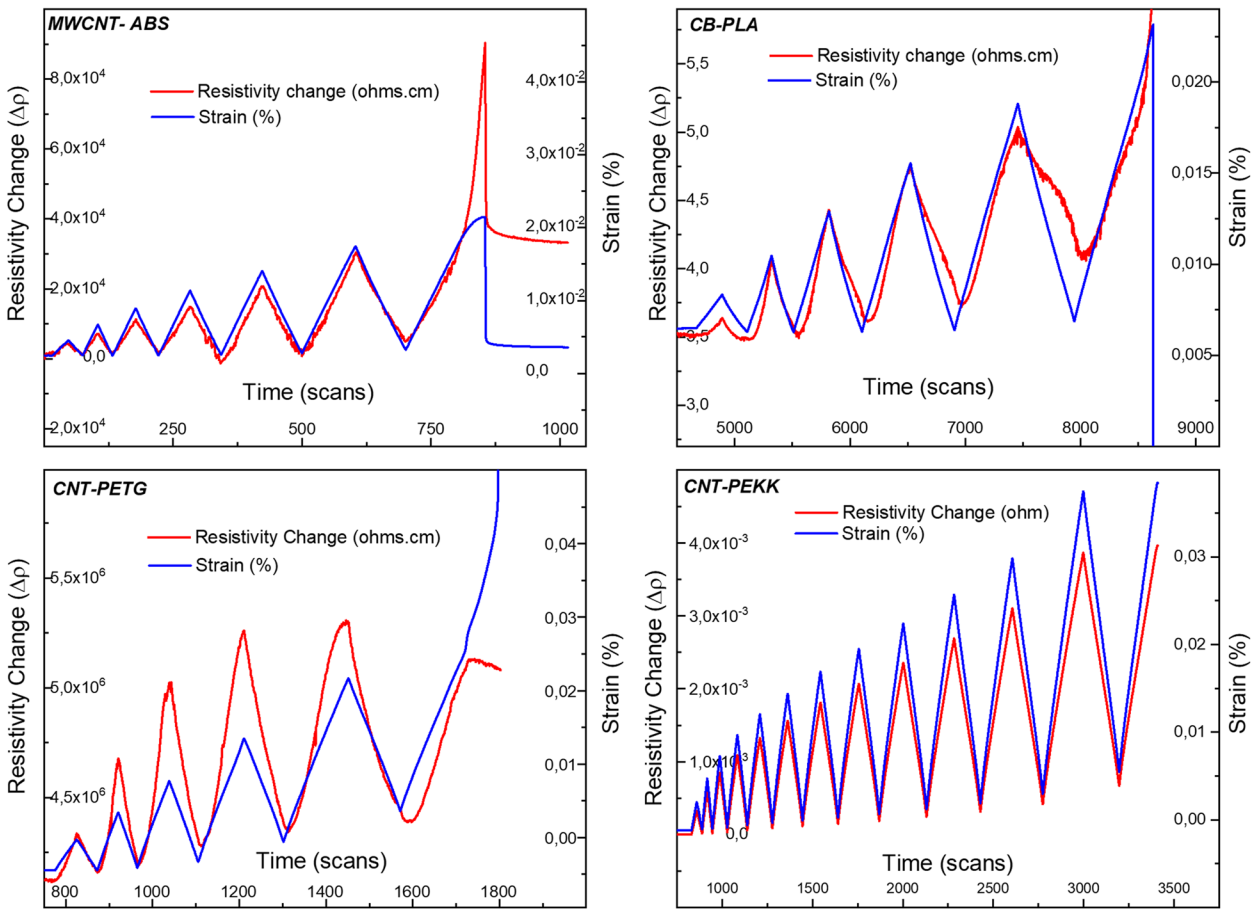

Fig. 3 Simultaneous measurements of resistivity change (red lines) and strain (blue lines) for conductive ABS, PLA, PETG and PEKK respectively

the resistivity changes before and after the production of the defect increases linearly with the gradual increase of size defect. For the window of hole size analyzed, a big range of resistivity is acquired which indicates that CNTs based epoxy resin is an excellent candidate for SHM, since even the smallest variation of defect size produces a clearly measured conductivity change. On the other hand, capability for strain detection was also evaluated by simultaneously measuring the variation of the strain and the variation of resistivity during a tensile test. The results, shown in Fig. 4c are very satisfactory: resistivity increases during deformation, and as soon as deformation ceases and the material returns to its original state, resistivity also decreases. Results shows good capability of this material for strain detection applications. In this case, the reason to observe the results plotted lies in the more brittle nature of resin matrix comparing with the thermoplastic showed in the previous point despite mechanical strength is like that corresponding to ABS, PETG or PLA. The main difference for this material is found in the curve corresponding to the resistivity change. When, after a load down, this curve does not reach the initial value (minimum initial value), it is assumed that microcracks start to appear in the microstructure of the material, giving rise to breakages in the CNTs conductivity changes. This damage is not reversible and accumulates after each load up cycle, which can be clearly seen in the increased value of resistivity change after each load down cycle ends. This effect is remarkably stronger for the case of the thermoset resin than for the thermoplastic due to its higher fragility.

Carbon fiber reinforced polymer composite

The study of evolution of conductivity properties with the increasing size of drilled hole reveals that this material does not respond well when defect-sizes are low (below 7 mm, see Fig. 5a). The reason behind these results lies in the fact that long fibers do not create percolation nets allowing strong conductivity changes, this explains the remarkable differences observed comparing with the two previous analyzed materials where a large easy to detect change of resistivity was produced by a breakage of a powerful conductivity chain even when small defects or strains are applied. By expanding the range of the defect size, its influence on the conductivity measurements begins to be noticed. This means that, for defects larger than 8 mm, this material is valid for SHM by the electrical resistivity method.

We simultaneously measured the variation in resistance between two electrodes separated by 5 cm, as well as the deformation generated in the specimen during a tensile test (Fig. 5b). Changes in resistivity were measured using electrodes and strain using strain gauges. The electrodes consist of silver paint directly on the previously sanded surface in the center of the specimen, then the crocodiles are placed and fastened with copper tape (note, the copper tape ends up coming loose). The gauges are placed symmetrically on both sides of the specimen between the electrodes with glue.

We have started to do cycles of loading and unloading that are clearly shown in graphs displayed in Fig. 5b. Three different phases might be distinguished: Phase 1: The resistance measurements at the beginning follow well those of tensile in phase and intensity. During this phase, at the end of the discharge cycle, the value of $\Delta R/l$ is zero. Phase 2: In phase 2, the first cracks appear and the permanent damage, therefore, at the end of the discharge cycles, $\Delta R/l$ always has a value other than zero due to the permanently open cracks (black dashed line). In this phase, the two signals (mechanical and resistive) also begin to shift. Phase 3: After the eighth cycle, the gauges stop measuring, it is assumed that there is a big damage produced in the resin until finally reach the breakage.

With the aim of evaluate failure location capacities of this material, measurements using a contacts configuration consisting of silver electrodes painted on the edges of the 20×20 cm specimen (picture of Fig. 5c): 5 pairs of electrodes on the X axis and 4 pairs of electrodes on the Y axis separated by 5 cm. Three holes located at the positions indicated in the drawing of Fig. 5e were made using a drill, two 1.5 cm in diameter and the other 2×1 cm.

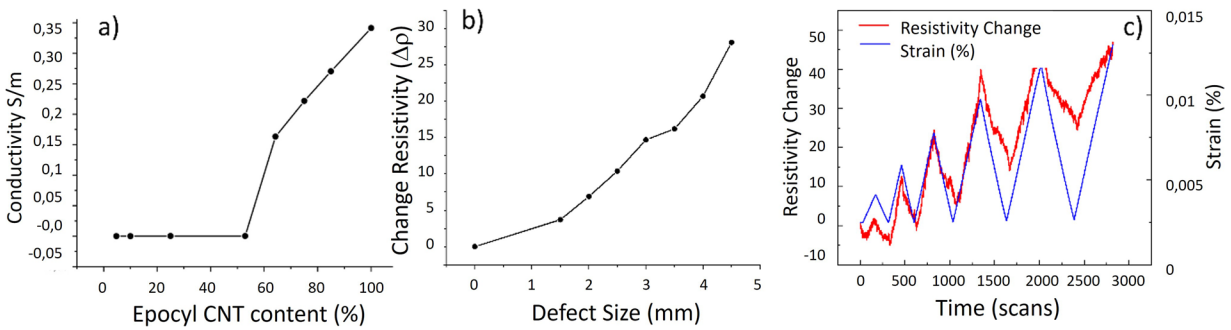

Fig. 4 **a**) Percolation curve of Epoxy resin blended with CNT- based Epoxy resin. **b**) Evolution of change of the resistivity with defect size. **c**) Simultaneous measurements of resistivity change (red lines) and strain (blue lines) for conductive epoxy resin

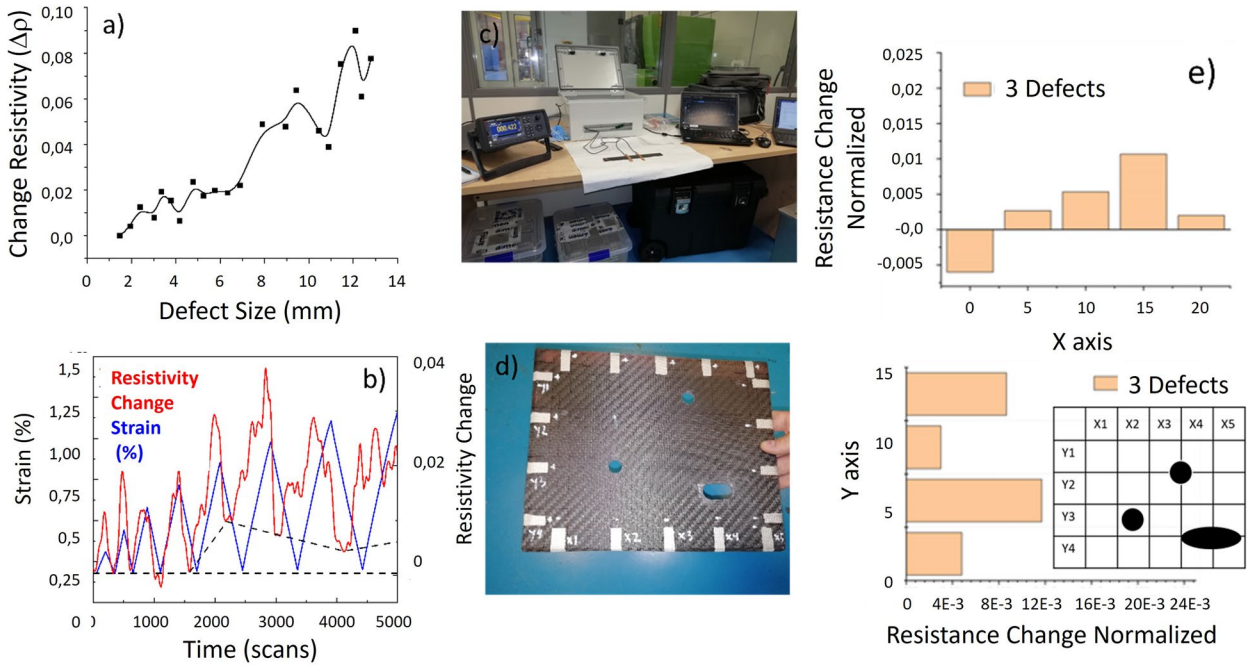

Fig. 5 **a**) Evolution of resistivity change with defect-size. **b**) Simultaneous measurements of resistivity change (red lines) and strain (blue lines). **c**) Picture of the resistivity measurements set up. **d**) Carbon fiber-based epoxy resin composite coupon prepared to evaluate failure detection capacities. **e**) measurements of resistivity change for different faced pairs of electrodes

Resistance values were measured for faced pair of contacts, results are displayed in bars graphics of Fig. 5e for pairs in X axis and Y axis. As explained, to obtain these values, pairs of opposite contacts were connected to the coupon in the position indicated in Fig. 5e separated by a determined distance, which is different for X and Y directions. This distance has an important effect in the measured resistance "contaminating" the effect produce by the size and position of the defect. For a correct evaluation of this method, it is important to remove this factor (distance between contacts) from the represented measurements normalizing the obtained value by a shape factor. In the case of coupons used in previous sections of the paper, coupons with well determined geometry, the shape factor is given by cross section of coupons and distance between contacts, as explained in experimental section. But in the case of a big coupon with several pair of contacts, the cross section is not easy to obtain. For this reason, normalized values of the change of the measured resistance are represented: direct ohmic resistance measured is divided by the distance between contacts (15 cm for X axis and 20 cm for Y axis). For positions where the resistivity change reaches higher values, a defect is assumed, and from values represented these graphics we can conclude that the material might self-detect the production and position of a defect of 2×1 cm located at X4Y4.

From all results explained above, important values have been estimated: Maximum stretch and Gauge factor (Table 4). These are very valuable to evaluate the capacity for strain sensing presented by the materials and to establish a comparison with other material solutions presented in literature.

Since we are presenting results corresponding to different composite families, some important aspects must be clarified. Concerning the maximum stretch achieved in each case the highest is the corresponding to the carbon fiber reinforce laminate. This result, absolutely expected, is due to important load of continuous carbon fiber reinforcement. Considering only the thermoplastic polymers, the most notable correspond to PEKK, high performance

Table 4 Values of Maximum stretch and Gauge factor corresponding to the different thermoplastic materials evaluated

Printed Material	Maximum stretch (MPa)	Gauge Factor
PLA	35	4,088 (0,018%)
ESD safe ABS	30	6,083 (0,018%)
CNT PETG	25	7,486 (0,018%)
PEKK-ESD	60	20,772
Epoxy resin with CNTs	30	90,011 (0,01%)
Carbon fiber reinforced polymer composite	460	0,086 (0, 2%)

thermoplastic due its mechanical properties and chemical stability. On the other side and considering the estimated Gauge Factor values, also is important to notice that the values obtained are given by different strain values depending on the nature of the composite evaluated, being epoxy resin and PEKK (among thermoplastic), both loaded with CNTs, the most promising materials for SHM and Strain detection applications. Finally, and as explained in previously, composite laminates based in long fibers does not present important potential to be applied to these ends.

Conclusions

In the presented work, electrical properties, and both damage and strain dependent electrical resistance characteristics of several different carbon-based/polymer composite and nanocomposite materials were investigated: (a) different carbon-based nano additives thermoplastic composite for 3D printing technologies: PLA/CB; ABS/CNTs; PETG/CNTs and PEKK/CNTs (b) CNTs reinforced RTM6 Epoxy resin and (c) long carbon fiber composite laminates.

All polymeric conductive composite and nanocomposite materials evaluated in this work present response to the formation of structural damage, being nanocomposite based in small amount of nanomaterials like CNTs the most sensitive and promised for applications in SHM.

All polymeric conductive composite and nanocomposite materials evaluated of different nature (thermoset and thermoplastic) have been proved suitable for applications in strain detection.

Long carbon fiber-based composites, allow to detect the production and the location of defects of 2×1 cm.

Abbreviations

NDI	Non-Destructive Inspections
SHM	Structural Health Monitoring
CNTs	Carbon nanotubes
FFF 3D	Fused Filament Fabrication three-dimensional
CB	Carbon Black

Acknowledgements

Works presented in this paper have been funded by the Spanish National Science and Technology Minister through the project READI (Ayudas Cervera para Centros Tecnológicos EXP—00122598 / CER-20191020) of the Red Cervera programms.

Authors' contributions

OSS has contributed to the presented work by manufacturing samples and carried out measurements of conductivity and tensile testing and carried out the preparation of the manuscript. DR has contributed to this work by manufacturing 3D printed samples. RL has contributed to this work by analysing results and supervising the work. ER has contributing to this work by supervising work and analysing result. The author(s) read and approved the final manuscript.

Funding

Works presented in this paper have been funded by the Spanish National Science and Technology Minister through the project READI (Ayudas Cervera para Centros Tecnológicos EXP—00122598 / CER-20191020) of the Red Cervera programm.

Availability of data and materials

The datasets used and/or analysed during the current study are available from the corresponding author on reasonable request.

Declarations

Competing interests

The authors declare no competing interests.

Author details

[1] Advanced Materials Department, AIMEN Technology Center, O Porriño, Spain.

Received: 25 November 2022 Accepted: 14 March 2023
Published online: 26 March 2023

References

1. K. Diamanti et al., Structural health monitoring techniques for aircraft composites tructures. Prog Aerosp Sci 46, 342–352 (2010)
2. M. Park et al., Strain-dependent electrical resistance of multi-walled carbon nanotube/polymer composite films. Nanotechnology. 19(5), 055705 (2008). https://doi.org/10.1088/0957-4484/19/05/055705. (7pp)
3. E.T. Thostenson et al., Real-time in situ sensing of damage evolution in advanced fiber composites using carbon nanotube networks. Nanotechnology. 19, 215713 (2008). https://doi.org/10.1088/0957-4484/19/21/215713. (6pp)
4. L. Gao et al., Sensing of Damage Mechanisms in Fiber-Reinforced Composites under Cyclic Loading using Carbon Nanotubes. Adv. Funct. Mater. 19, 123–130 (2009). https://doi.org/10.1002/adfm.200800865
5. J.-M. Park et al., Inherent sensing and interfacial evaluation of carbon nanofiber and nanotube/epoxy composites using electrical resistance measurement and micromechanical technique. Composites: Part B 38, 847–861 (2007)
6. C Viets, et al. Damage mapping of GFRP via electrical resistance measurements using nanocomposite epoxy matrix systems. Composite part B. 2013. dx.doi.org/https://doi.org/10.1016/j.compositesb.2013.09.049.
7. http://www.eco-compass.eu/context-2
8. R. Zhang et al., Strain sensing behaviour of elastomeric composite films containing carbon nanotubes under cyclic loading. Compos Sci Technol 74, 1–5 (2013)
9. Katsunori Suzuki. Rapid-response, Widely Stretchable Sensor of Aligned MWCNT/Elastomer Composites for Human Motion Detection.2016. DOI: https://doi.org/10.1021/acssensors.6b00145
10. Conor S Boland et al. Sensitive, High-Strain, High-Rate Bodily Motion Sensors Based on GrapheneRubber Composites. 2017. (DOI: https://doi.org/10.1002/adfm.201606604).
11. Hongfei Zhu. Versatile Electronic Skins for Motion Detection of Joints Enabled by Aligned Few-Walled Carbon Nanotubes in Flexible Polymer Composites.2017. DOI: https://doi.org/10.1002/adfm.201606604
12. D. Xiang et al., Enhanced performance of 3D printed highly elastic strain sensors of carbon nanotube/thermoplastic polyurethane nanocomposites via non-covalent interactions. Composites Part B Eng 176, 107250 (2019). https://doi.org/10.1016/j.compositesb.2019.107250
13. B. Podsiadły et al., Electrically Conductive Nanocomposite Fibers for Flexible and Structural Electronics. Appl. Sci. 12, 941 (2022). https://doi.org/10.3390/app12030941
14. J..F. Christ et al., 3D printed highly elastic strain sensors of multiwalled carbon nanotube/thermoplastic polyurethane nanocomposites. Mater Des 131, 394–401 (2017). https://doi.org/10.1016/j.matdes.2017.06.011
15. C. Luan et al., Fabrication and characterization of in situ structural health monitoring hybrid continuous carbon/glass fiber–reinforced thermoplastic composite. Int J Adv Manuf Technol 116, 3207–3215 (2021). https://doi.org/10.1007/s00170-021-07666-3
16. Md. Fazlay Rabbi et al. Strain and damage sensing in additively manufactured CB/ABS polymer composites, Polymer Testing, Volume 90, 2020, 106688, ISSN 0142-9418, https://doi.org/10.1016/j.polymertesting.2020.106688

Publisher's Note